



Figures and figure supplements

Regulation of posterior body and epidermal morphogenesis in zebrafish by localized Yap1 and Wwtr1

David Kimelman *et al*

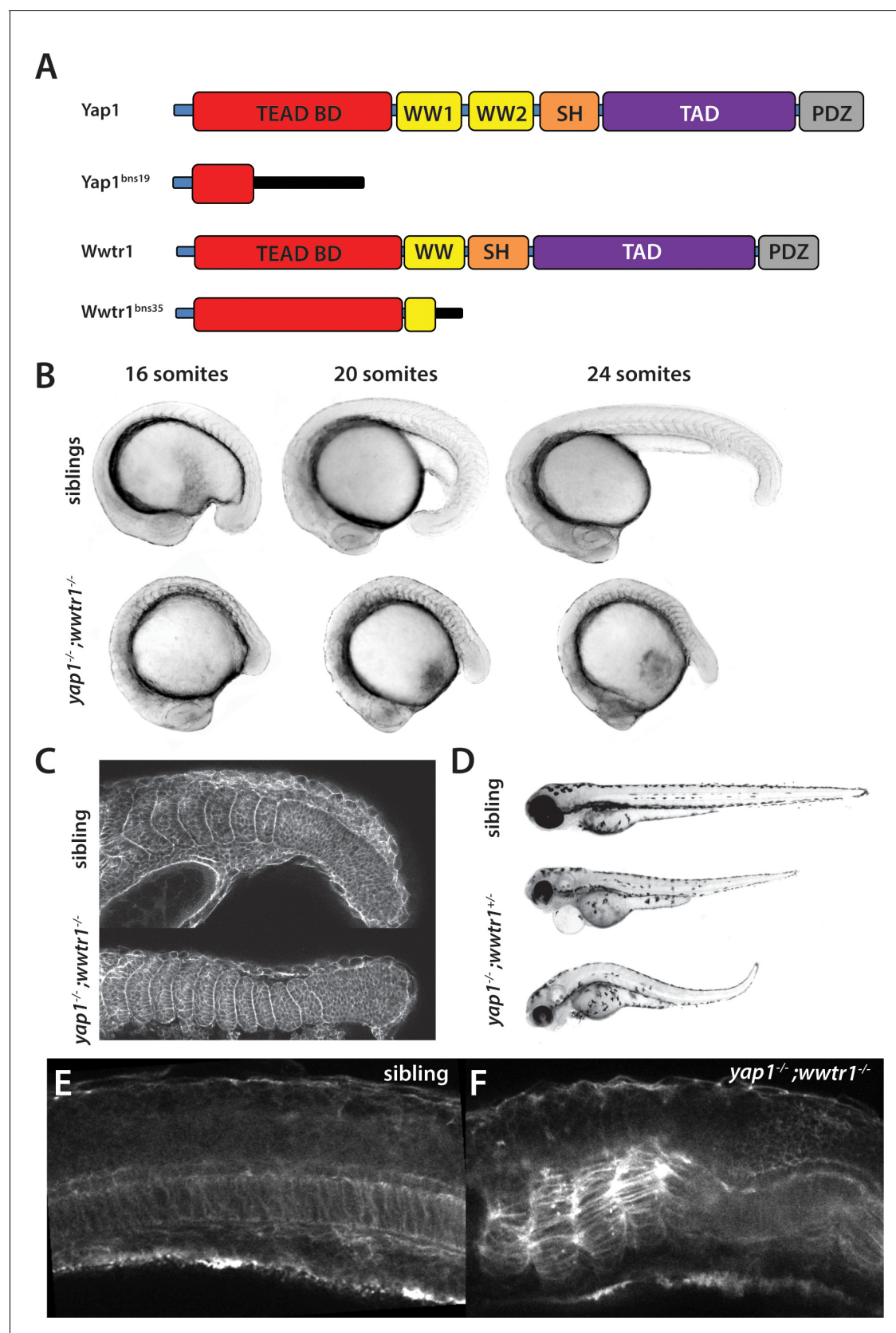


Figure 1. *yap1;wwtr1* double mutants exhibit severely altered posterior development. (A) Schematic showing the two mutants used in this work. TEAD BD is the TEAD binding domain, TAD is the Transcriptional Activation Domain, and WW, SH and PDZ are protein interaction domains. The black bar

Figure 1 continued on next page

Figure 1 continued

indicates new sequence following the frame shift caused by the mutation. (B) Time course showing the development of the posterior body defect in *yap1;wwtr1* double mutants. The same sibling and double mutant embryos are photographed at all three stages. (C) Phalloidin staining shows that the somites form in the mutants but never acquire the chevron shape found in wild-type embryos. 24-somite stage (21 hpf) embryos, anterior to the left. (D) Embryos with a *yap1*^{-/-};*wwtr1*^{+/-} genotype show a milder posterior body defect at 72 hpf (n = 15). Pericardial edema is also variably present. (E,F) Midline confocal sections of the trunk with somite 1 on the left side of a sibling (E) and a *yap1;wwtr1* double mutant embryo (F) at the 24-somite stage.

DOI: <https://doi.org/10.7554/eLife.31065.002>

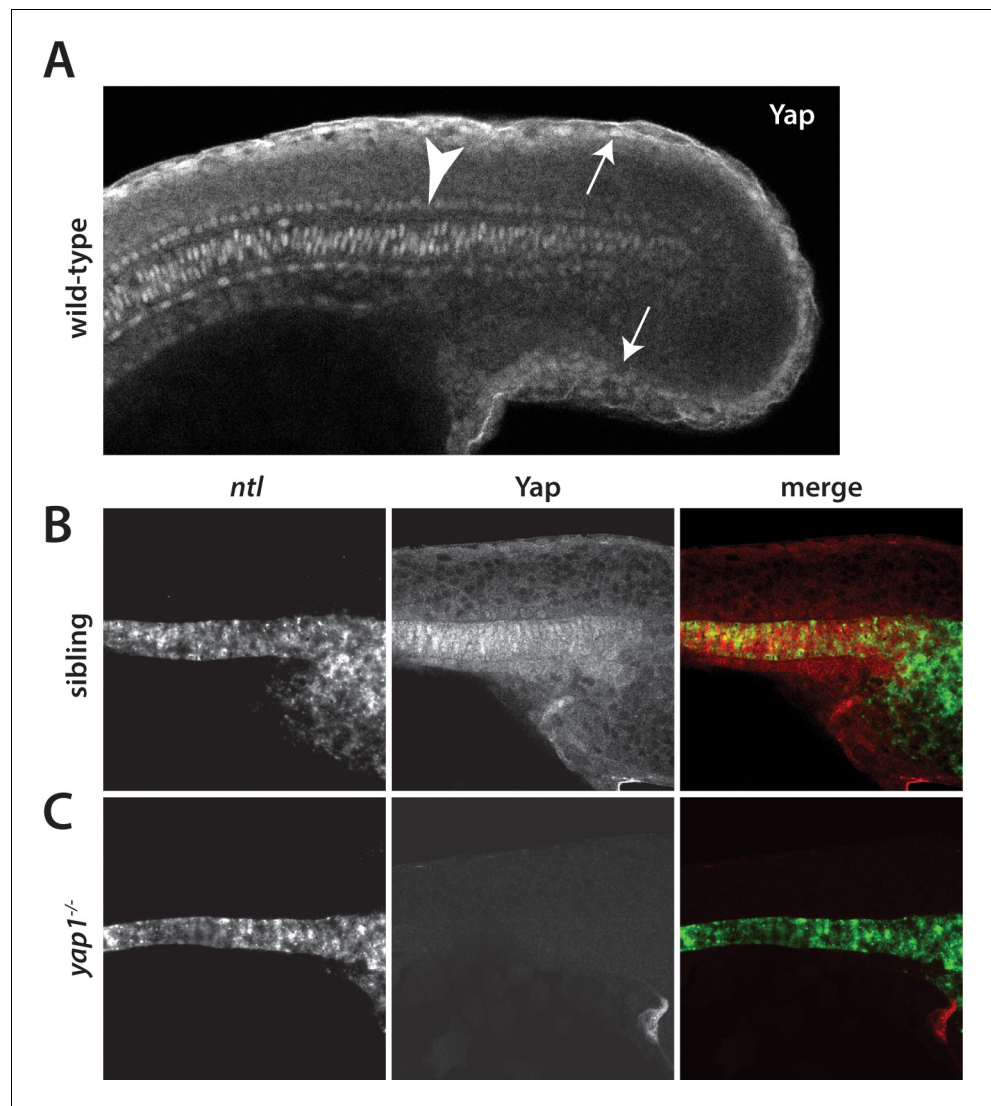


Figure 2. Yap1 is localized to the presumptive epidermis and axis. (A) Yap1 protein is expressed in the presumptive epidermis (arrows) and midline (arrowhead) of an 18-somite stage embryo. (B) Co-stain with the notochord marker *no tail* (*ntl*), in green, using FISH demonstrates Yap1 expression, in red, in the notochord. (C) No reactivity with the Yap1 antibody was observed in *yap1*^{-/-} mutant embryos. Note that the longer Proteinase K digestion used in the standard FISH protocol reduced the presumptive epidermal Yap1 staining. All embryos are at 18 somites with anterior to the left.

DOI: <https://doi.org/10.7554/eLife.31065.004>

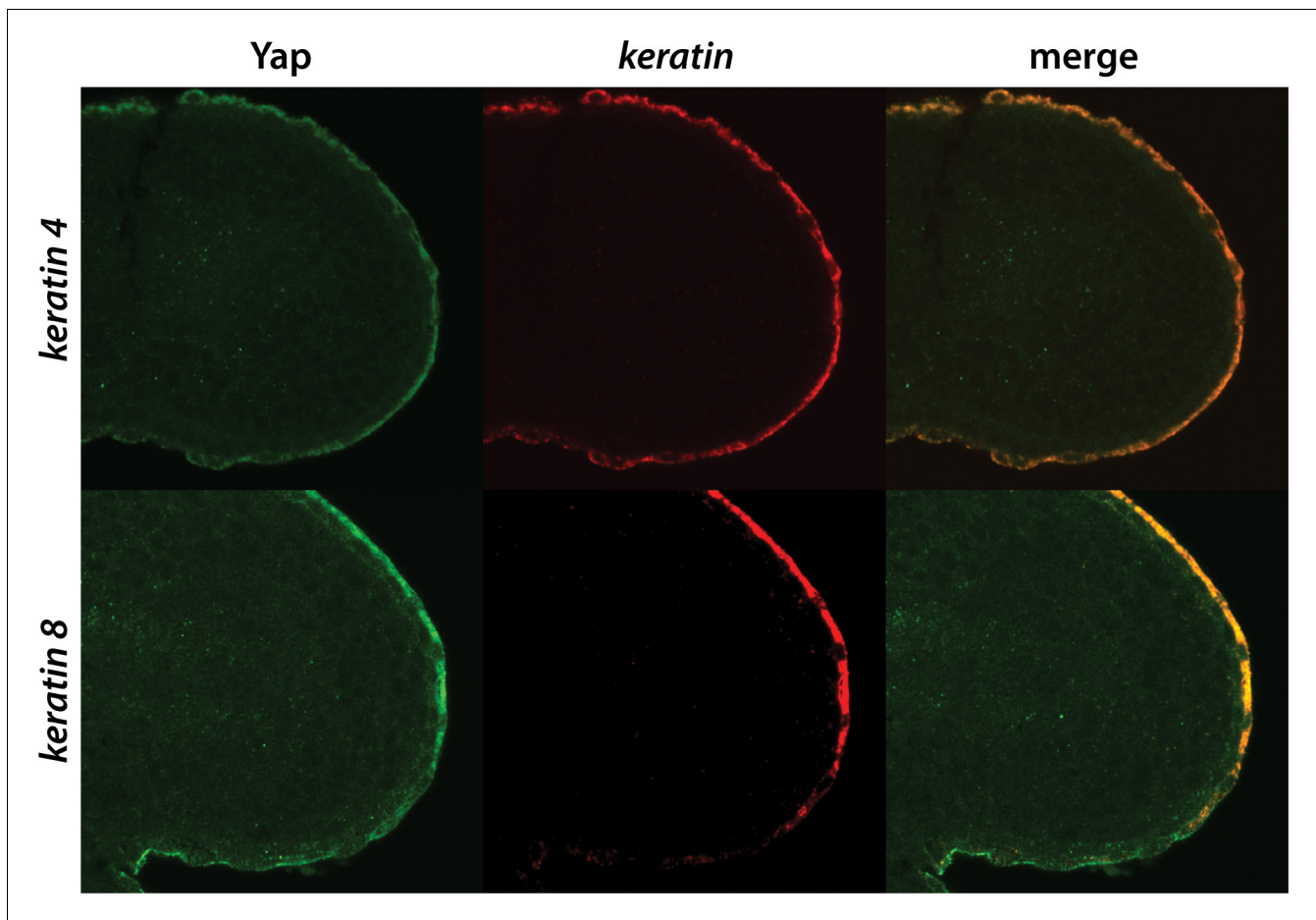


Figure 2—figure supplement 1. Yap1 localizes to the presumptive epidermis. A combination of FISH and immunofluorescence was used to co-stain embryos for Yap1 protein and *keratin 4* or *keratin 8* mRNA, which are restricted to the presumptive epidermis. A brief (5 min) Proteinase K step was used for the FISH, which preserves the presumptive epidermal Yap1 stain but does not allow for strong notochord staining.

DOI: <https://doi.org/10.7554/eLife.31065.005>

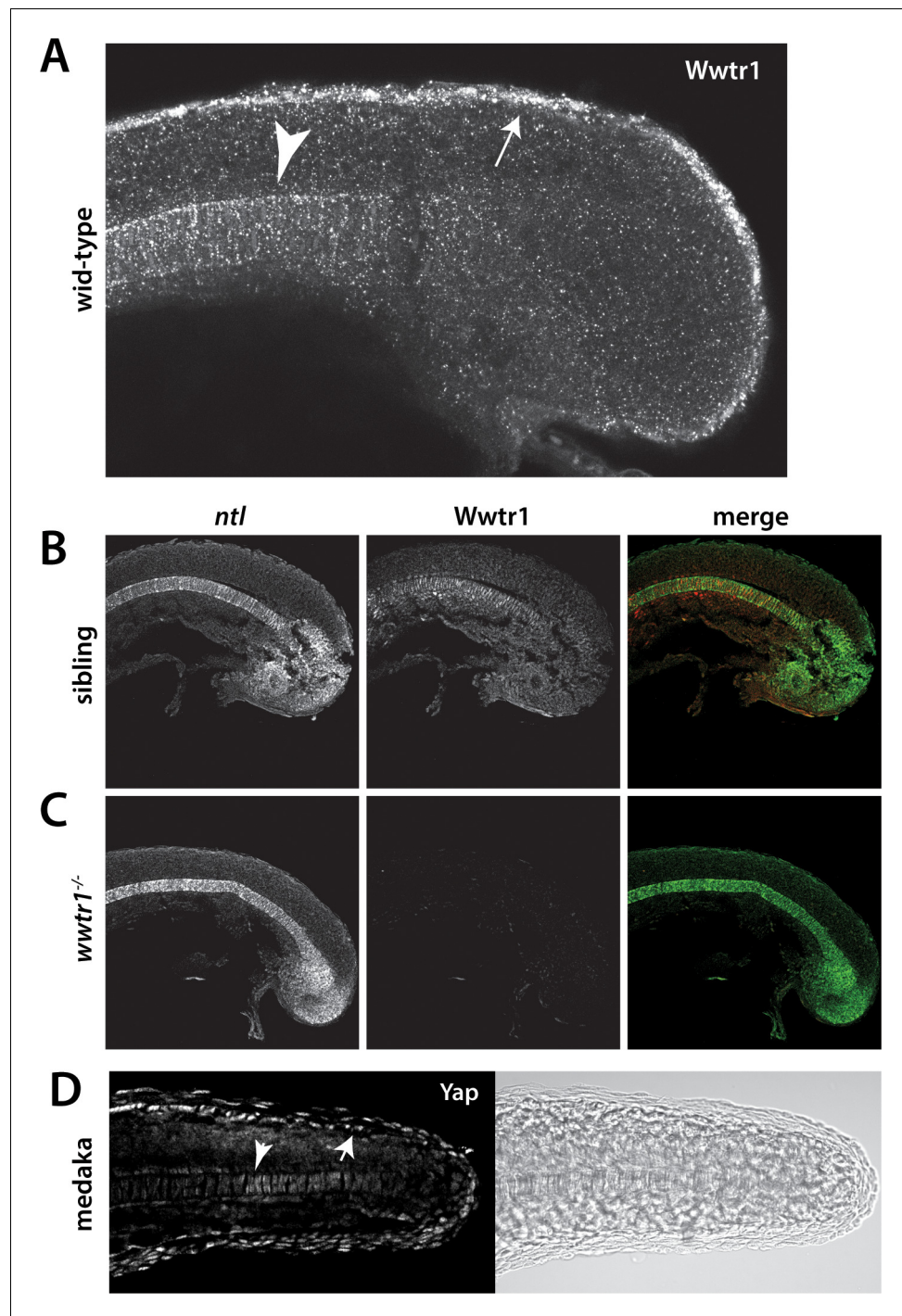


Figure 2—figure supplement 2. Wwtr1 and medaka Yap1 localize to the presumptive epidermis and notochord. (A–C) Wwtr1 expression in zebrafish embryos. Wwtr1 is expressed in the presumptive epidermis (arrow) and notochord (arrowhead) of an 18-somite embryo (A). Co-stain with the notochord marker *no tail* (*ntl*) (in green) demonstrates Wwtr1 expression (in red) in the notochord (B). No reactivity with the anti-Wwtr1 antibody was observed in *wwtr1* mutant embryos (C). All embryos are 18 somites with anterior to the left. (D) Yap1 is expressed in the presumptive epidermis (arrow) and notochord (arrowhead) of an 18-somite medaka embryo.

DOI: <https://doi.org/10.7554/eLife.31065.006>

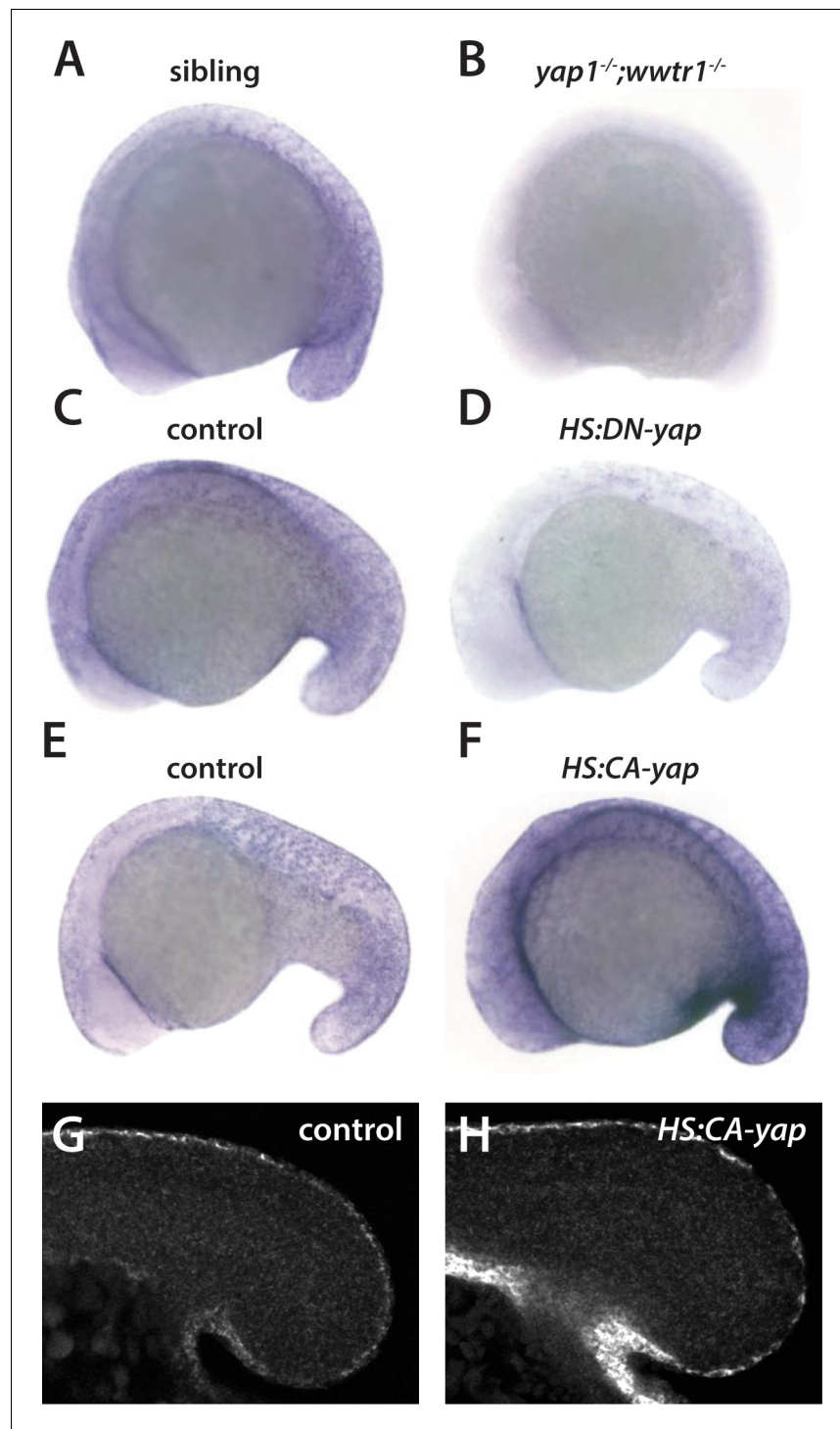


Figure 3. Regulation of *ecrg4b* expression by Yap1 and Wwtr1. (A,B) *ecrg4b* is expressed in the presumptive epidermis of sibling embryos (A) but is not expressed in *yap1*;*wwtr1* double mutant embryos (B). (C–F) Transgenic embryos obtained from an outcross of hemizygous *HS:DN-yap* or *HS:CA-yap* adults were heat shocked at the 4-somite stage and then raised to 18 somites. The genotype of the embryos was determined by PCR after the in situ hybridization to be either transgenic or non-transgenic control. Expression of DN-yap decreased *ecrg4b* expression relative to non-transgenic controls (C,D, n = 6 for each) whereas CA-yap enhanced *ecrg4b* expression (E,F, n = 4 for each). (G,H) Embryos analyzed using FISH probe to *ecrg4b* demonstrates that CA-yap increases expression of *ecrg4b* only in the epidermis (n = 4 for each). All embryos are at the 18-somite stage.

DOI: <https://doi.org/10.7554/eLife.31065.008>

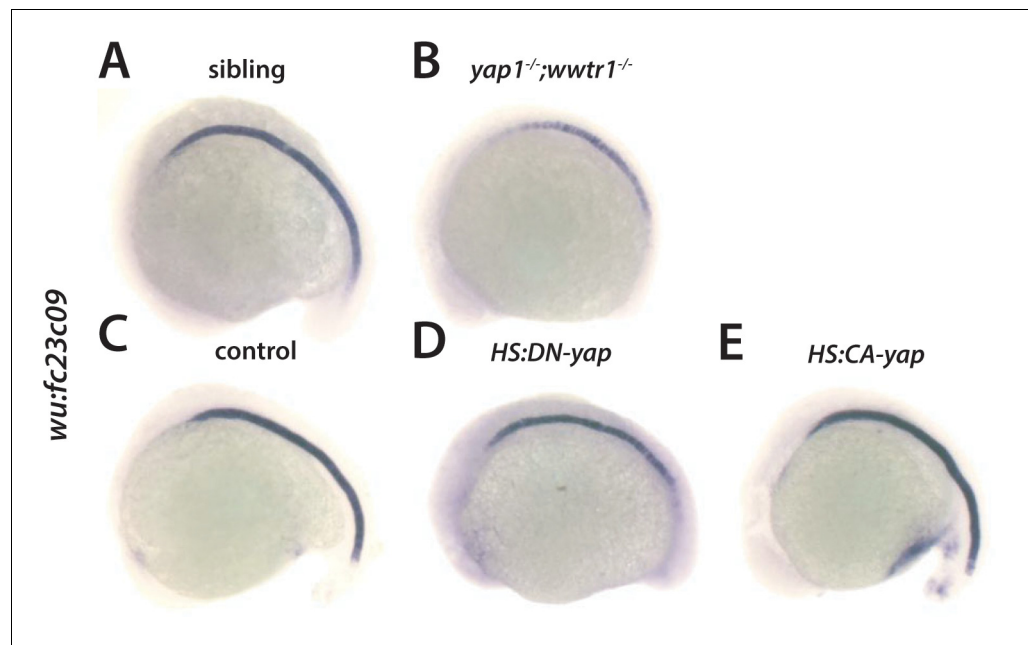


Figure 3—figure supplement 1. Regulation of *wu:fc23c0* by Yap1 and Wwtr1. (A,B) *wu:fc23c0* is strongly expressed throughout the notochord of sibling embryos (A) but not expressed in the posterior notochord of *yap1*; *wwtr1* double mutant embryos. (C–E) Transgenic embryos obtained from an outcross of hemizygous *HS:DN-yap* or *HS:CA-yap* adults were heat shocked at the 4-somite stage and then grown to 18 somites. The genotype of the embryos was determined by PCR after the in situ hybridization to be either transgenic or non-transgenic control. Expression of DN-yap decreased posterior notochord *wu:fc23c0* expression (D, n = 10) whereas CA-yap did not appear to alter *wu:fc23c0* expression (E, n = 8) relative to control non-transgenic embryos (C).

DOI: <https://doi.org/10.7554/eLife.31065.009>

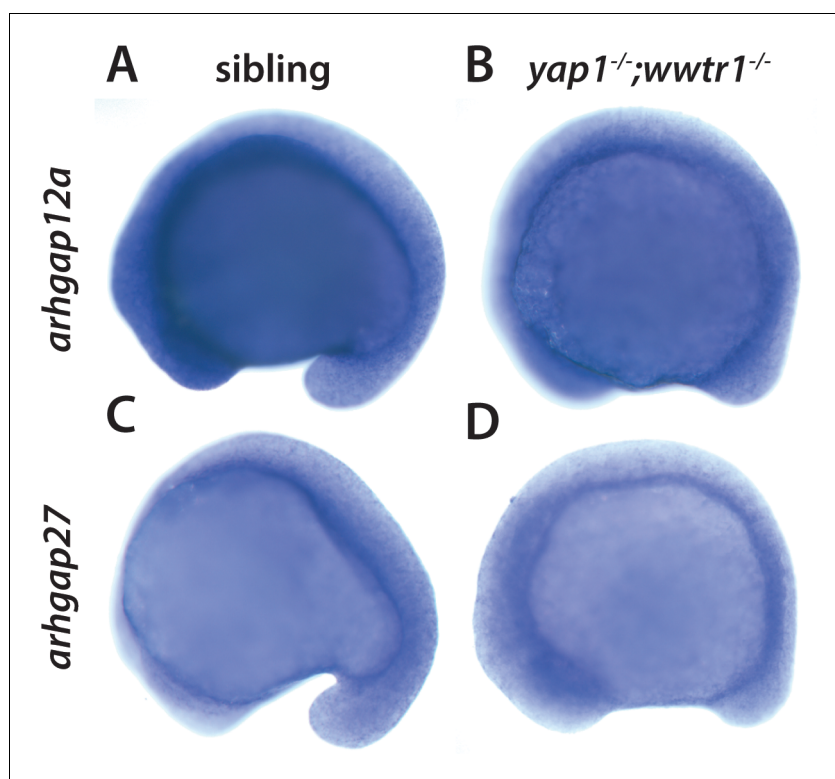


Figure 3—figure supplement 2. Yap1 and Wwtr1 do not regulate *arhgap12* and *arhgap27* expression. (A,B) *arhgap12a* and (C,D) *arhgap27* are expressed in the presumptive epidermis at the same level in sibling and *yap1*; *wwtr1* double mutant embryos. The yolk is blue from the prolonged development times necessary to visualize these weakly expressed transcripts.

DOI: <https://doi.org/10.7554/eLife.31065.010>

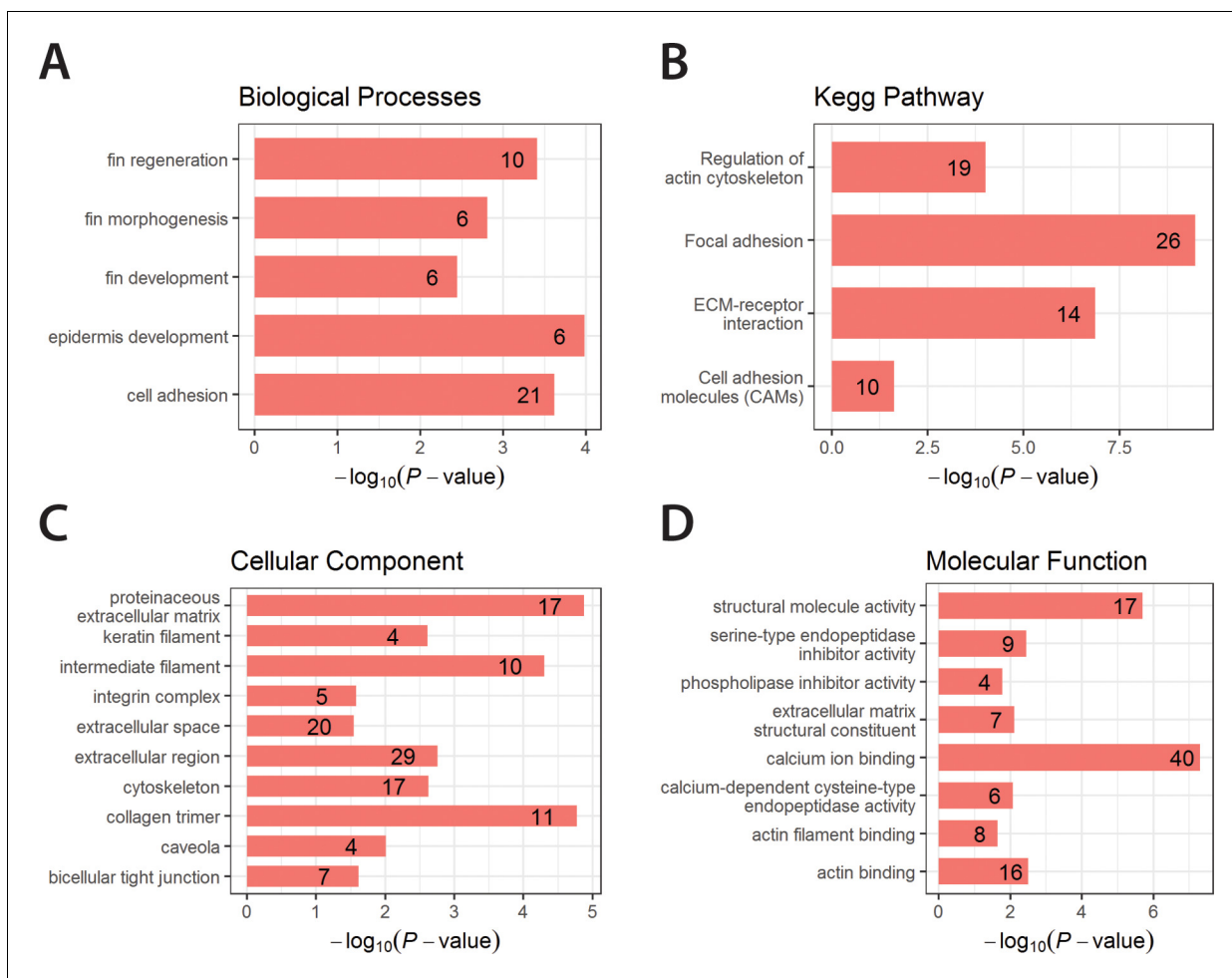


Figure 4. Enriched GO terms and Kegg Pathway for downregulated genes in *yap1;wwtr1* double mutants. Bar graphs showing the log-transformed adjusted *P*-values of enriched GO terms categorized under Biological Processes (A), Cellular Component (C) and Molecular Function (D), and for the Kegg Pathway (B). Number of genes in the enriched terms is shown in respective bar graphs.

DOI: <https://doi.org/10.7554/eLife.31065.011>

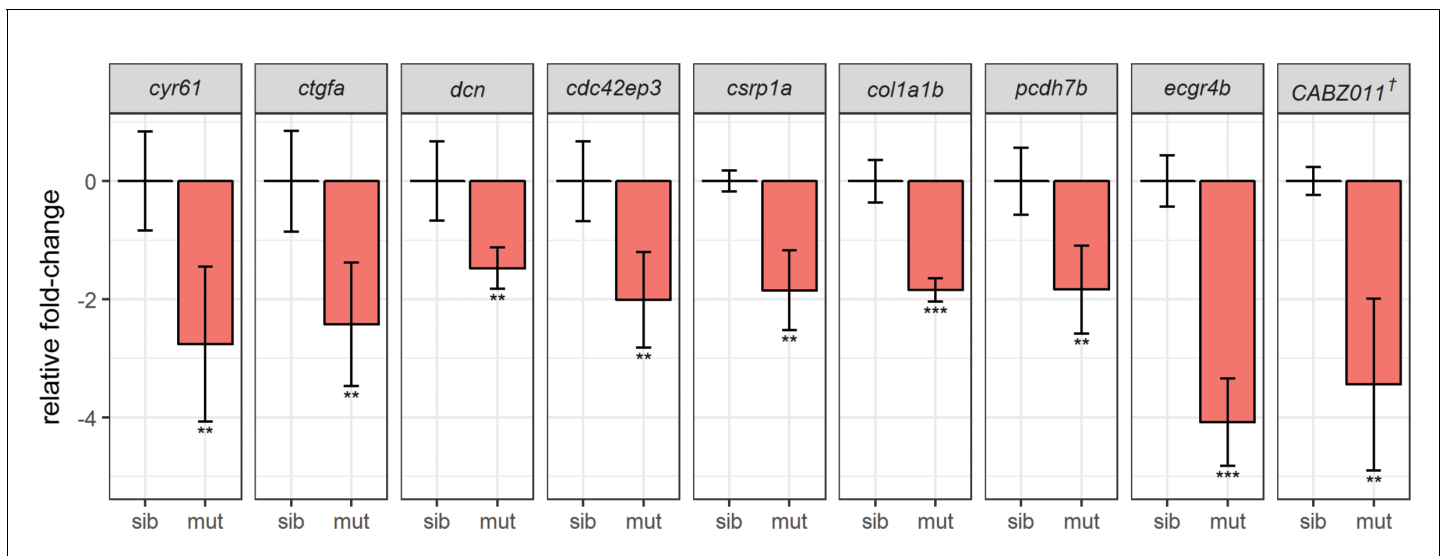


Figure 4—figure supplement 1. Real-time PCR (qPCR) assays validate downregulation of known Yap1/Wwtr1 target genes. Tail buds from siblings and *yap1;wwtr1* double mutants were collected in the same manner as in the RNA-seq experiment, and sample genes from **Tables 1** and **2** were assessed. All genes assessed were from four biological replicates (sib: $n = 4$; mut: $n = 4$) except *csrp1a* (sib: $n = 4$; mut: $n = 3$). The Cq values were normalized to *rp13* and are provided in **Supplementary file 2**. The graphs represent mean \pm s.d. *P*-values were calculated by one-tailed two-sample t-test and corrected for multiple hypotheses testing (FDR method). * - $p < 0.05$; ** - $p < 0.01$; *** - $p < 0.001$. sib – siblings; mut – mutants. † - CABZ01115881.1.

DOI: <https://doi.org/10.7554/eLife.31065.012>

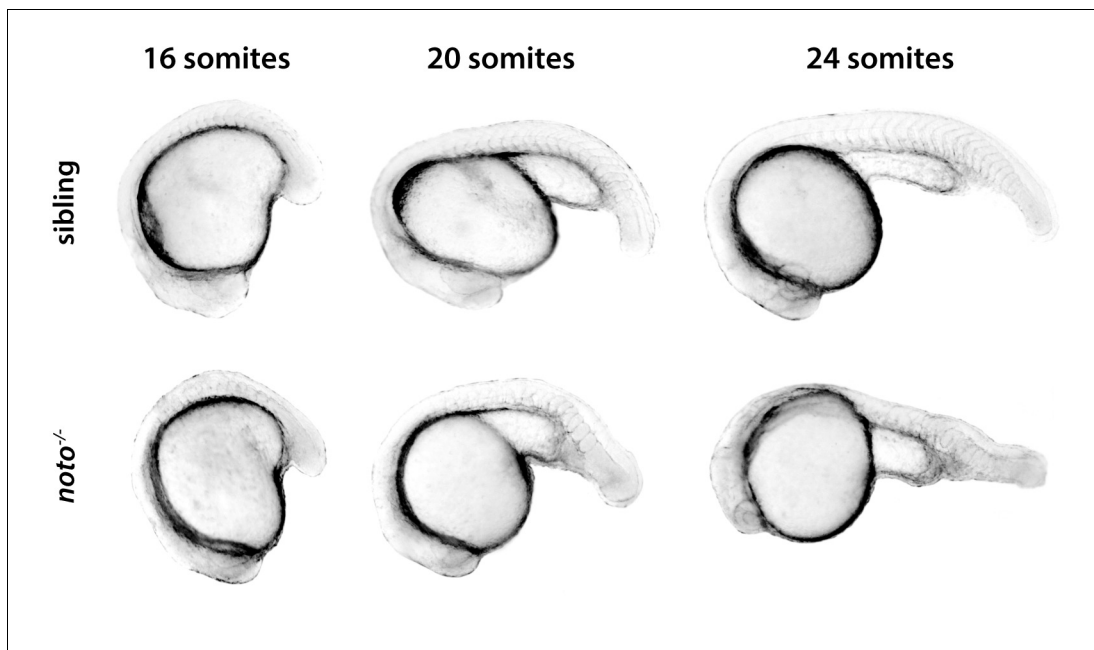


Figure 4—figure supplement 2. Morphogenetic defects in *noto* mutants. Embryos from a cross of *noto*ⁿ¹ heterozygotes were sorted at the 16-somite stage when the *noto* phenotype first becomes visible. The same sibling and mutant embryos are photographed at all three stages shown.

DOI: <https://doi.org/10.7554/eLife.31065.013>

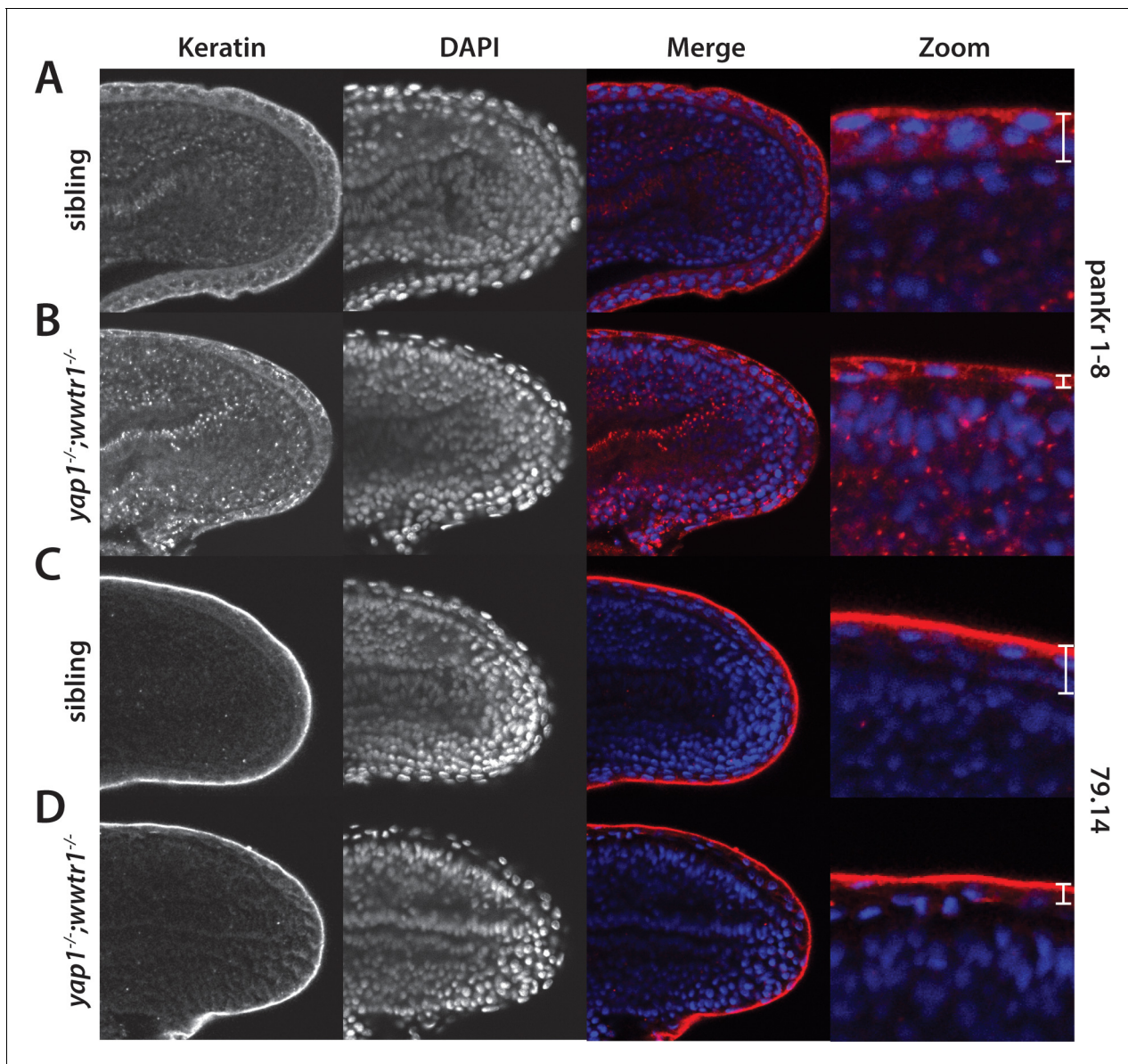


Figure 5. Alterations in the presumptive epidermis in *yap1;wwtr1* double mutants. Mutant and sibling embryos at the 24-somite stage were fixed, incubated with the anti-keratin antibodies panKr1-8 (A,B) or 79.14 (C,D), and then co-stained with DAPI. Confocal images of the midline of the tailbud, with anterior to the left. Note the thinner presumptive epidermis in the mutants compared to that in the siblings.

DOI: <https://doi.org/10.7554/eLife.31065.015>

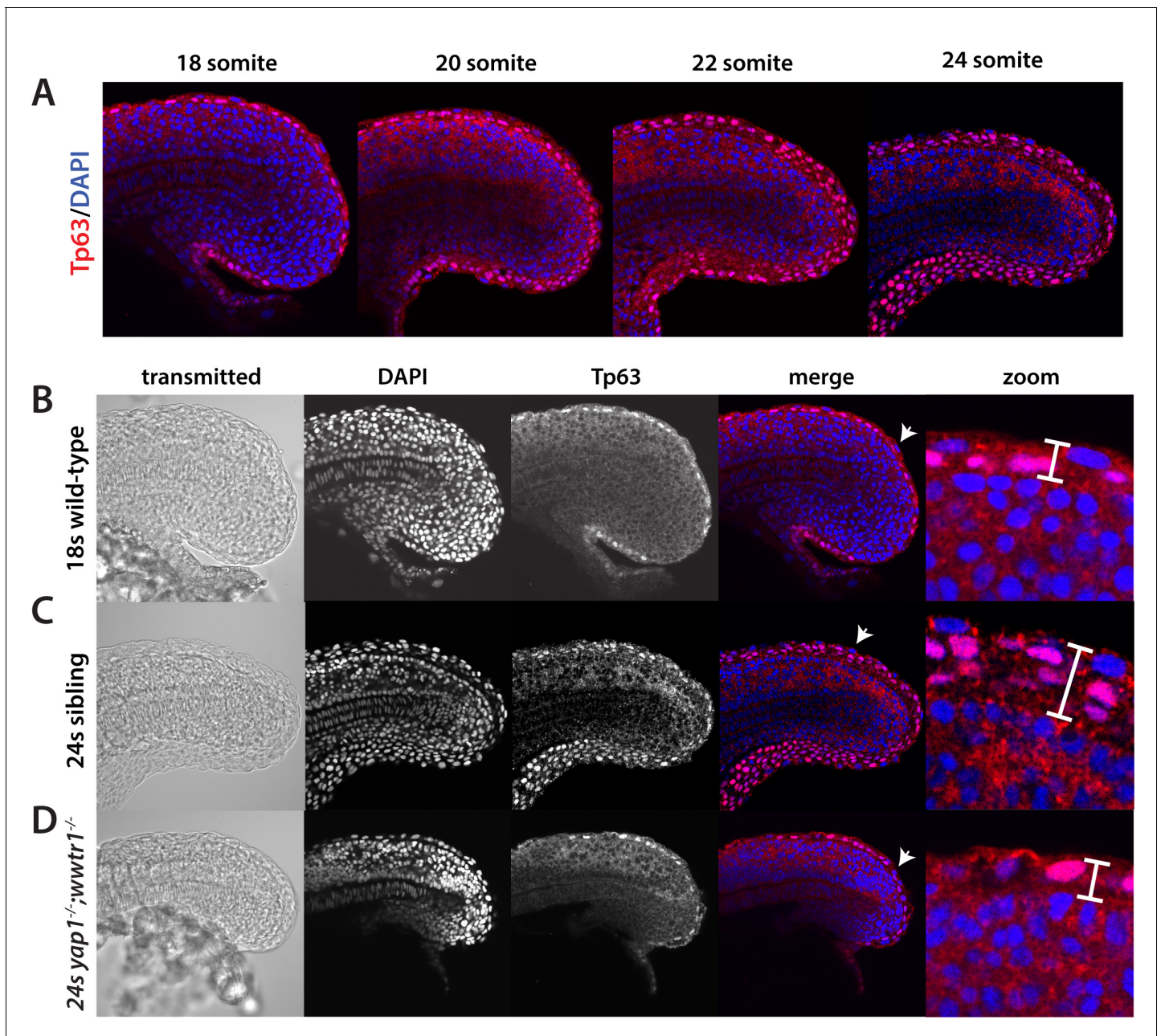


Figure 6. Tp63 positive cells accumulate at the nascent fin fold in sibling but not mutant embryos. Embryos were incubated with the anti-Tp63 antibody, and then co-stained with DAPI. (A) Embryos were collected at the indicated stages. Note the increase in Tp63-positive cells on the dorsal and ventral midline as the embryos age. (B–D) The Tp63-positive presumptive epidermis at the 18-somite stage (B) is one layer thick, but increases to multiple layers by the 24-somite stage in sibling (C) but not in *yap1*;*wwtr1* double mutant embryos (D). Confocal images of the midline of the tailbud, with anterior to the left. The zoomed in images in panels B–D are of the dorsal side, and the arrows in the merged images point to the rare presumptive epidermis Tp63-negative cells.

DOI: <https://doi.org/10.7554/eLife.31065.016>

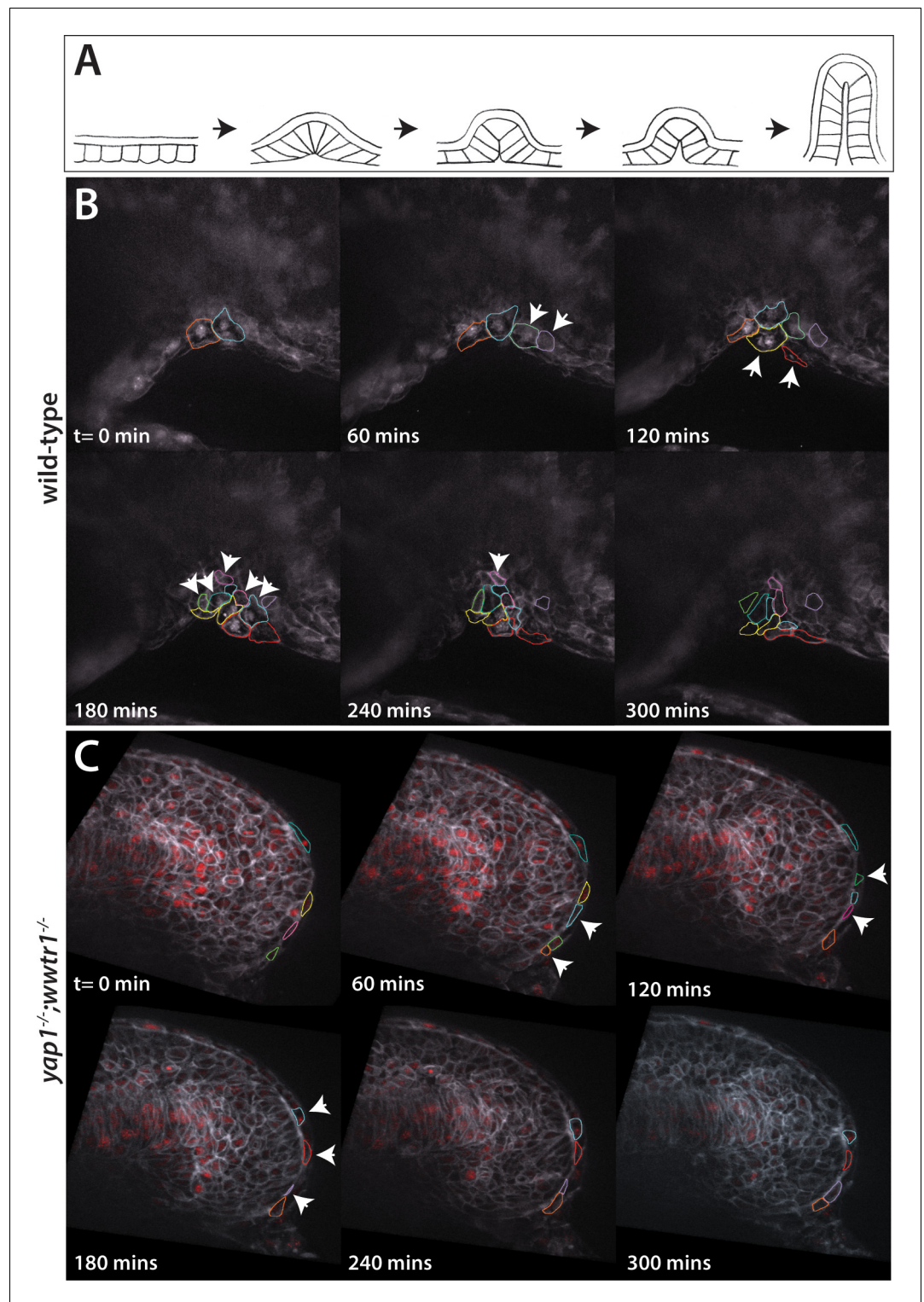


Figure 7. Dynamic movements of presumptive epidermal cells at the ventral fin fold. (A) Cartoon showing previous analysis of dorsal fin fold formation redrawn from *Dane and Tucker, 1985*. (B) Stills from live imaging of ventral fin fold formation in wild-type embryos taken from *Video 2*. (C) Stills from live imaging of ventral fin fold formation in *yap1*; *wwtr1* double mutants taken from *Video 3*. Images are of the midline with anterior to the left. Arrowheads point to new cells arriving at the midline. Most of the cells in the wild-type arrive basally, although two cells outlined appear at the edge of the fin fold coming from the other side of the embryo. Note that in wild-type

Figure 7 continued on next page

Figure 7 continued

embryos most cells that are at the midline at $t = 0$ min, or come to the midline at later times, stay at the midline whereas in the *yap1;wwtr1* double mutants cells are frequently transiently at the midline (quantified in **Figure 8**). Lateral views of the ventral-posterior part of the embryo, with dorsal up and ventral down. Wild-type movie is a representational movie of 21 movies examined and the mutant movie is representational of 11 movies.

DOI: <https://doi.org/10.7554/eLife.31065.017>

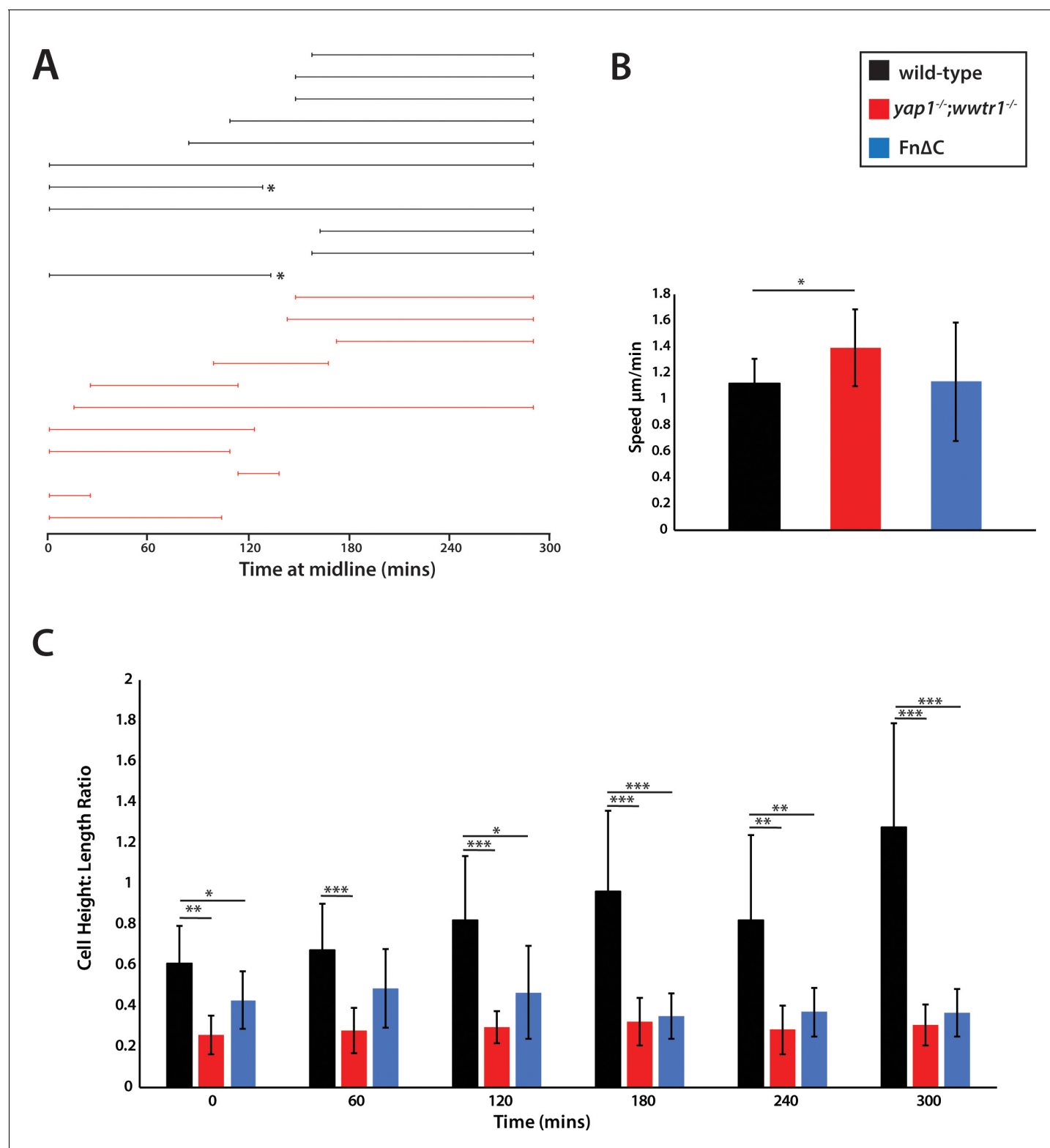


Figure 8. Measurements of presumptive epidermal cells at the ventral fin fold. (A) The time individual cells were at the midline measured in a single movie each for wild-type cells and *yap1;wwtr1* double mutant cells. Embryos were positioned on their side and filmed from the left side. When mutant cells crossed over the midline to the right side of the embryo, we stopped recording them, resulting in a truncated line. Note that while it was obvious when mutant cells left the midline because the epidermis is thin in these embryos, it was not completely clear in two of the wild-type cases (asterisks) whether cells left the midline or if they were obscured by other cells in the accumulating fin fold. (B) Movement speed for presumptive epidermal wild-type cells. (C) Cell height to length ratio for presumptive epidermal cells. *Figure 8 continued on next page*

Figure 8 continued

type cells, *yap1;wwtr1* double mutant cells, and cells expressing FnΔC, all measured at the midline. (C) Height-Length ratio of individual presumptive epidermal cells at the midline, taken at various time points during the filming of an individual movie. Height is a measurement of the apical-basal distance, and length is measured as the distance along the body axis. For both panels B and C, each column in the graph represents the average of 10 cells. * $p < 0.05$; ** $p < 0.01$; *** $p < 0.001$.

DOI: <https://doi.org/10.7554/eLife.31065.018>

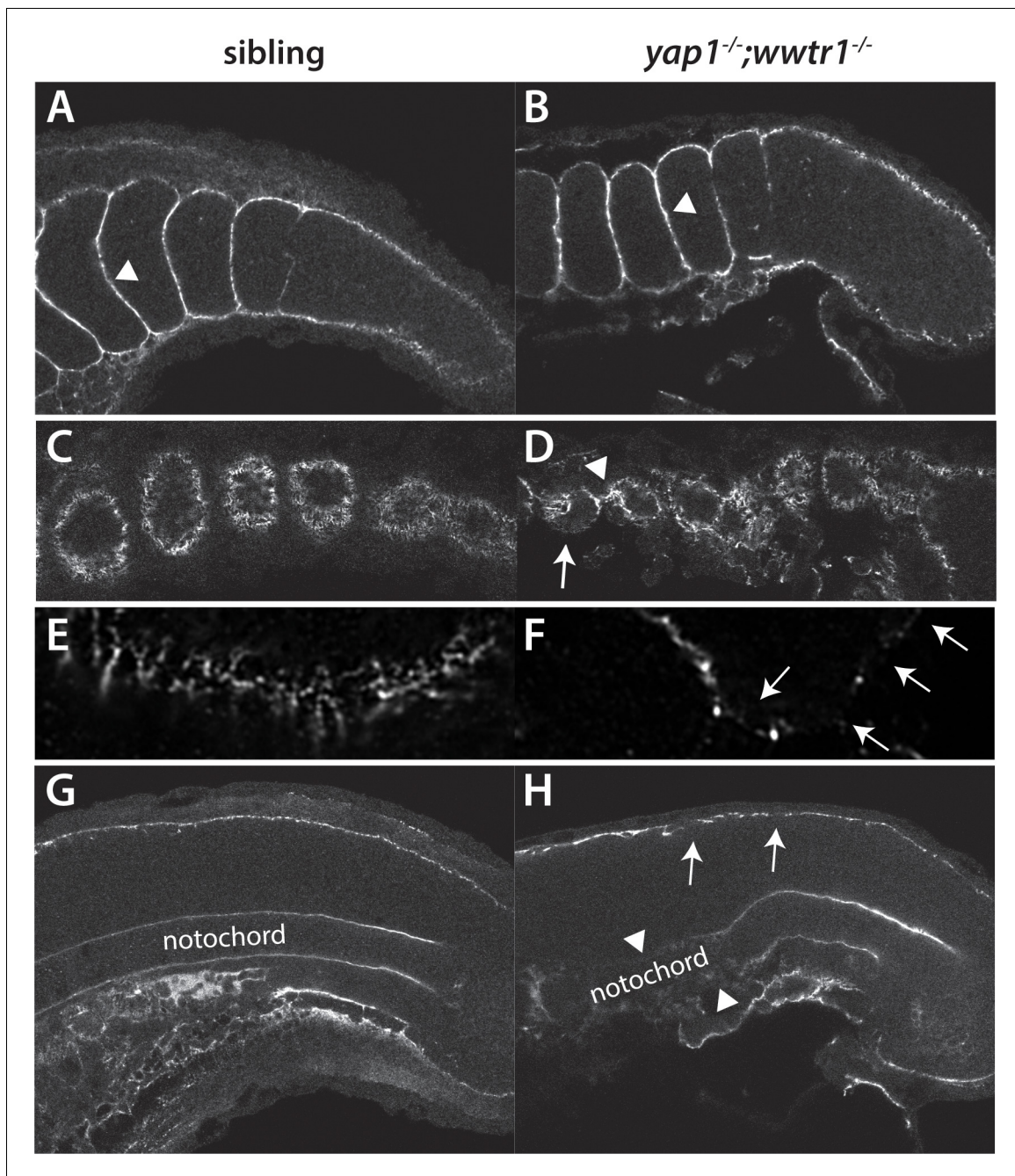


Figure 9. Fibronectin deposition is altered in *yap1;wwtr1* double mutants. (A,B) Intersomitic Fn deposition (arrowheads) appears unaffected in sibling and mutant embryos. Lateral confocal section. (C,D) At the lateral edges of the somites, Fn is present in rosettes where the somites contact the presumptive epidermis in sibling embryos (C), whereas in *yap1;wwtr1* double mutants there are gaps (arrow) and regions of enhanced Fn accumulation (arrowhead, (D)). (E, F) Higher magnification views of the ventral region of a single somite near its lateral edge from sibling (E) and *yap1;wwtr1* double mutant (F) embryos showing altered Fn accumulation in the mutants. Arrows point to gaps in Fn deposition. (G,H) At the midline, Fn is discontinuous underneath the presumptive epidermis in *yap1;wwtr1* double mutants (arrows, (H)) compared to siblings (G)). The posterior notochord Fn staining appears mostly unaffected in *yap1;wwtr1* double mutants, whereas in more anterior regions the Fn staining is absent (arrowheads), unlike in the siblings. All embryos are at 18-somites with anterior to the left.

DOI: <https://doi.org/10.7554/eLife.31065.021>

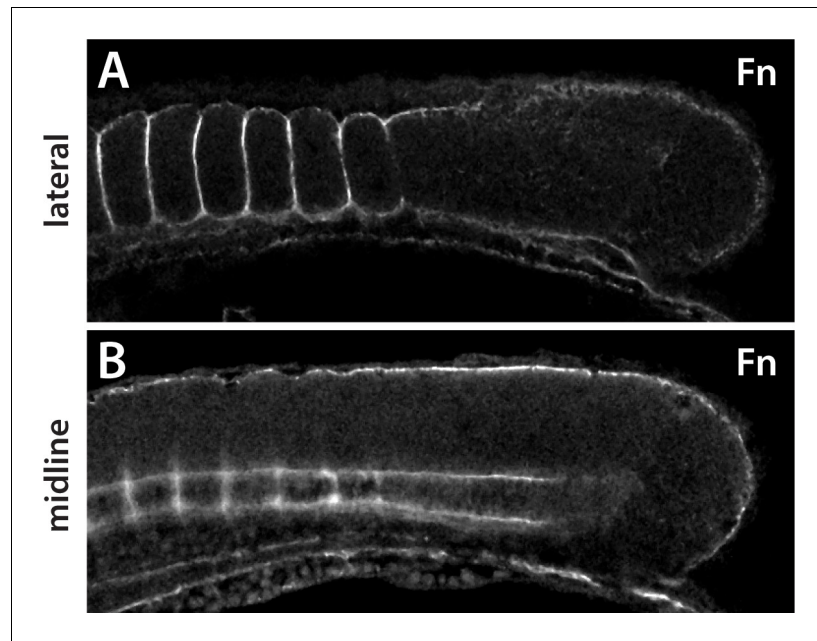


Figure 9—figure supplement 1. Expression of Fn in medaka embryos. (A) In a lateral section Fn protein is observed around the somites, including between adjacent somites, but does not appear within the somites as is also observed in zebrafish. (B) In a midline section, Fn is observed under the epidermis and around the notochord, as in zebrafish. Fn is also observed in periodic clusters along the notochord in medaka.

DOI: <https://doi.org/10.7554/eLife.31065.022>

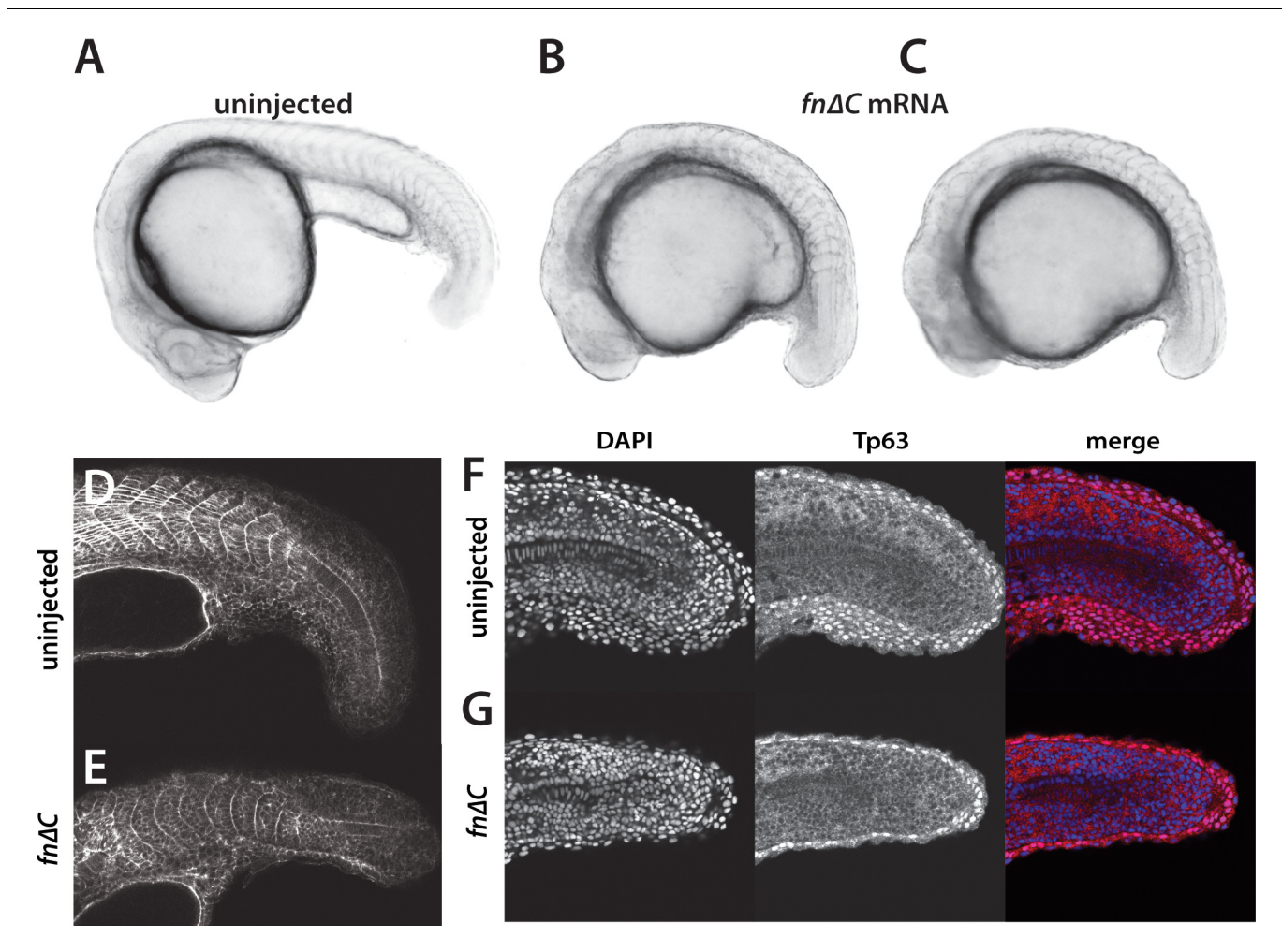


Figure 10. Inhibition of Fibronectin activity mimics the *yap1;wwtr1* double mutant phenotype. (A–C) Control embryo (A) and embryos injected with 400 pg *fnΔC* mRNA (B,C). (D, E) Control (D) and *fnΔC*-injected (E) embryos stained with phalloidin. Note the absence of chevron-shaped somites in panel E. (F, G) Control (F) and *fnΔC*-injected (G) embryos incubated with the anti-Tp63 antibody and co-stained with DAPI. Note the single layer of Tp63-positive presumptive epidermal cells in panel G ($n = 12/12$ embryos with a shortened tail had a single layered presumptive epidermis). All embryos are at the 24-somite stage with anterior to the left.

DOI: <https://doi.org/10.7554/eLife.31065.023>

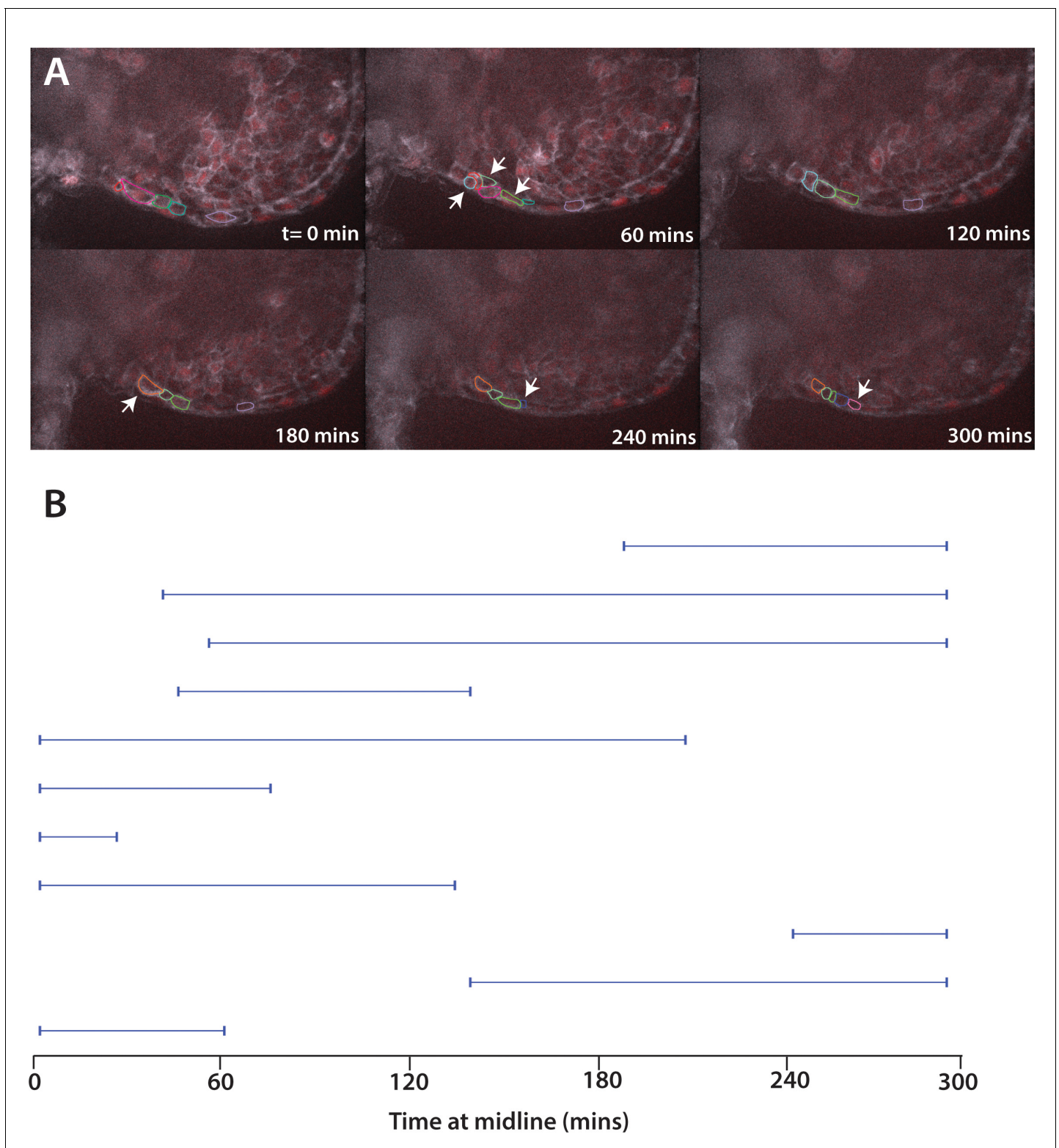


Figure 10—figure supplement 1. Movement of cells expressing FnΔC. (A) Stills from live imaging of ventral fin fold formation in embryos expressing FnΔC from injected mRNA. This movie is a representational movie of one of three movies. Arrowheads show new cells entering the fin fold. (B) The time individual FnΔC expressing cells were at the midline measured in a single movie. Compare to wild-type cells in **Figure 8A**. Embryos were positioned on their side and filmed from the left side. When FnΔC cells crossed over the midline to the right side of the embryo, we stopped recording them, resulting in a truncated line.

DOI: <https://doi.org/10.7554/eLife.31065.024>

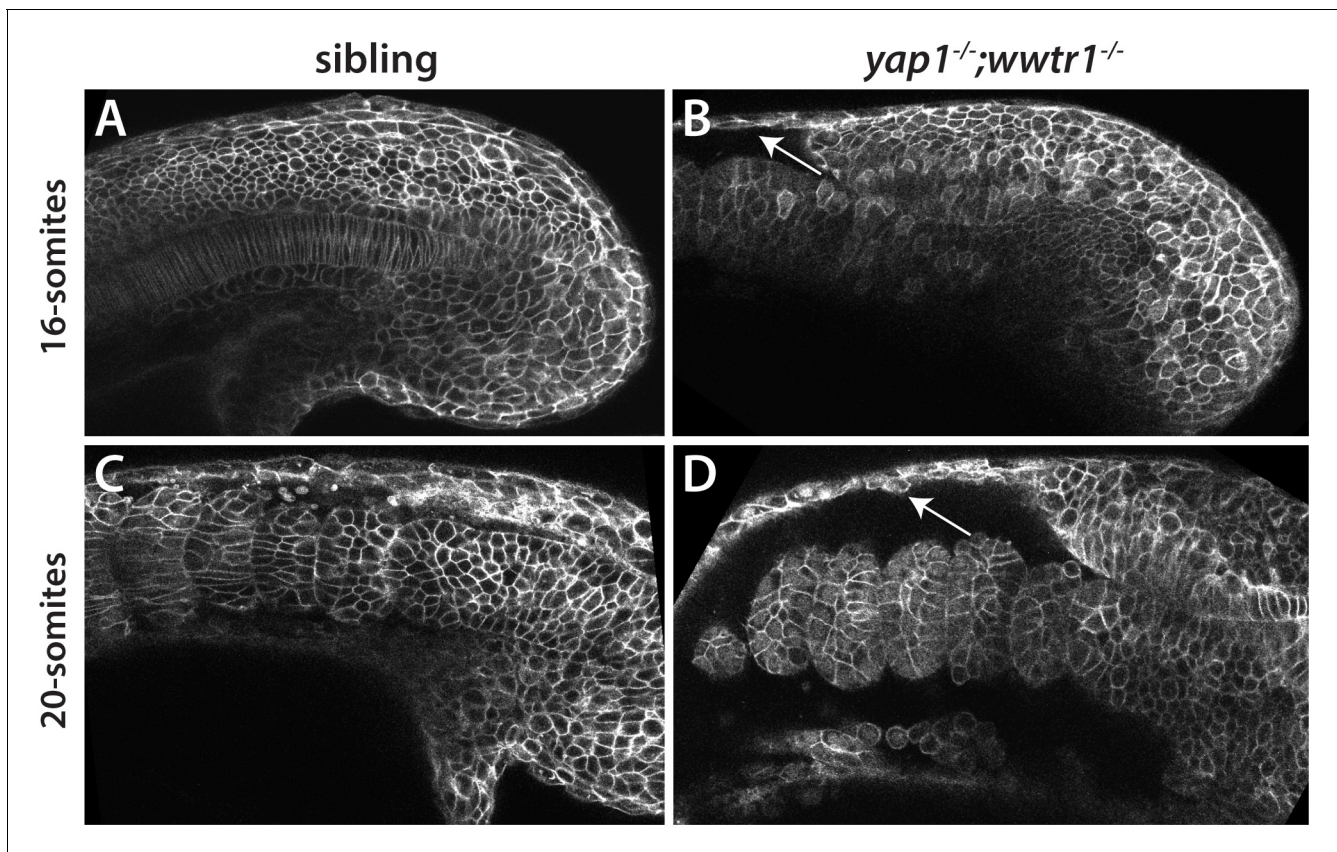


Figure 11. Reduced adhesion of presumptive epidermis in *yap1*;*wwtr1* double mutants. (A–D) Embryos were injected with mRNA encoding a membrane-localized form of GFP and imaged at the indicated stages. (A,C) Sibling embryos. (B,D) *yap1*;*wwtr1* double mutant embryos. Note the progressive separation of the epidermis from the somites (arrows), which increases from the 16-somite to the 20-somite stage. Four of four mutant embryos at the 16-somite stage exhibited the tissue separation phenotype and three of three at the 20-somite stage.

DOI: <https://doi.org/10.7554/eLife.31065.026>

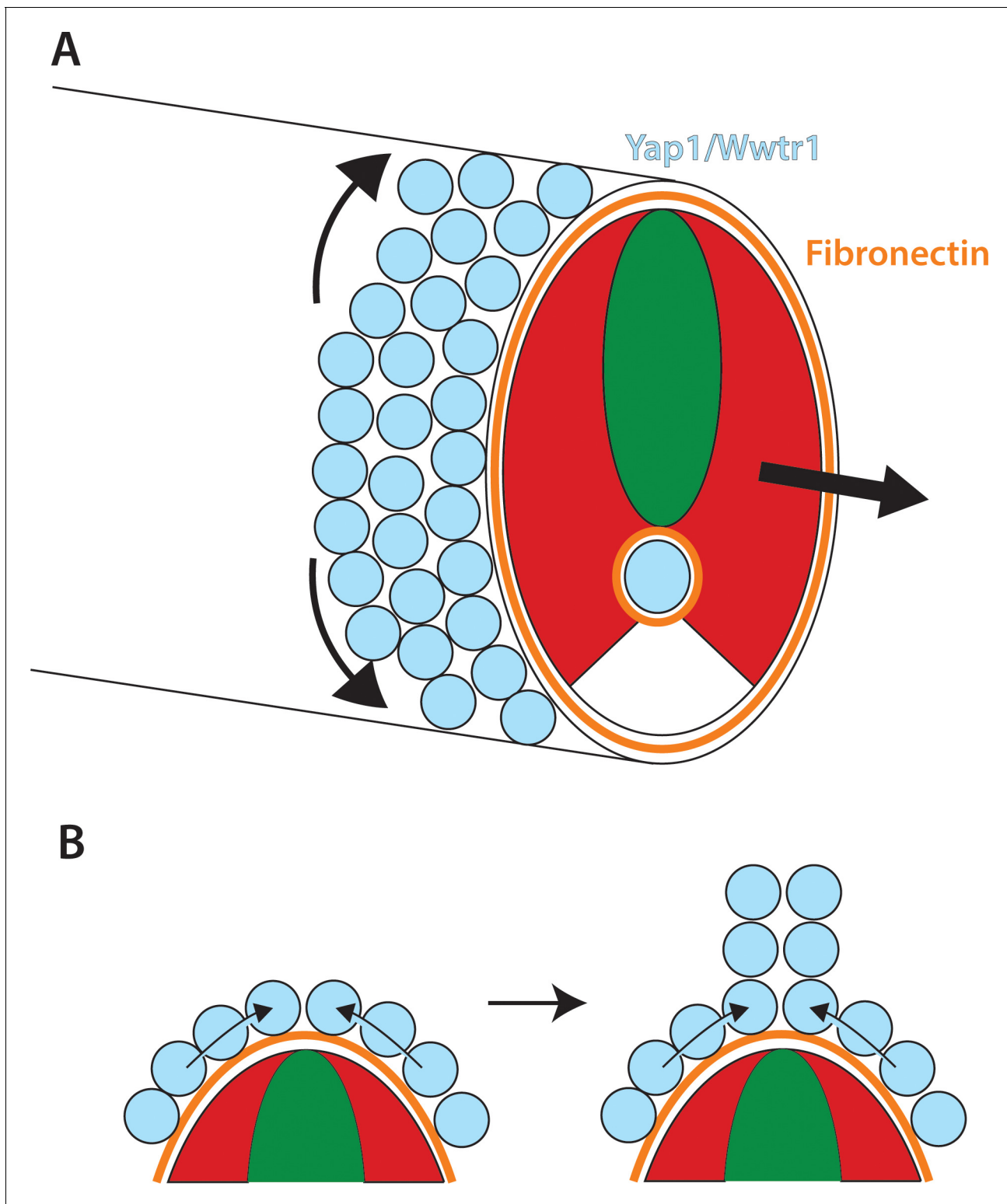


Figure 12. Role of Yap1/Wwtr1 in somite stage morphogenesis. (A) Yap1 and Wwtr1 are expressed specifically in the presumptive epidermis and notochord (light blue), where they promote cell adhesion and Fn assembly (orange). These processes are essential for both the movement of presumptive epidermal cells dorsally and ventrally to form the MFF, and for force transmission of the underlying tissues to allow the elongation of the posterior body. (B) At the midline, cells are converging from either side and push against each other to form the dorsal (shown) and ventral MFFs. We propose that adhesion to Fn is required for cells to be able to create the necessary force to allow them to generate the MFF. The presomitic mesoderm is shown in red and the neural tube is green.

DOI: <https://doi.org/10.7554/eLife.31065.027>